Dominik POCIECHA, Paweł ŻYŁKA
DEPARTMENT OF ELECTRICAL ENGINEERING FUNDAMENTALS, WROCLAW UNIVERSITY OF TECHNOLOGY,
27 Wybrzeże Wyspiańskiego, 50-370 Wrocław, Poland

The histogram-enhanced Hough transform applied to automated readout of analogue gauge meters using digital image processing

Abstract

The paper presents a computer vision technique developed for automated reading of analogue gauge meters. The system utilizes a mobile phone digital camera for image stream capturing and the Hough transform supplemented by multiply histogram analysis for locating a pointer position and parallax effect correction. The system is capable of working with minimal user supervision and its indicator position detection uncertainty is superior to that provided by a human eye. An attempt to use the algorithm implementation for semi-automatic calibration of an analogue voltmeter is also presented.

Keywords: metrology, computer vision, digital image processing.

1. Introduction

Computer-based automation of processes is nowadays a common practice, especially in the case of activities that are repetitious, tedious, complex and time consuming. Calibration of measuring devices is an example of such a process, normally involving a highly-skilled human operator to allocate the standard value, inspect the calibrated device reading and work out the calibration records. Most of measuring devices manufactured today are digital in nature and have at least one digital interface making communication with a control equipment (commonly a personal computer) thus measurement as well as calibration data exchange straightforward. Usage as well as calibration of such devices is less human-demanding and may be thus easily computerized. There are even available specialized calibrators (e.g. Fluke 9500B) making automated digital oscilloscope calibration possible and multifunction calibrators (e.g. Fluke 75x) designed to work with a broad range of sensors (e.g. those with built-in HART protocol).

On the other hand, there are still in use many high-quality analogue indicator measuring devices which do not have any digital interface making the automatic process of their readout (and thus calibration) impossible through direct data exchange. In such a case, there are still applicable manual methods in which laboratory staff must perform visual readout as well as the complete calibration procedure, consisting of several series of standard value fixing, readout taking and calculation of results. Such tasks are not only time consuming but also prone to errors because of a "human factor" involvement in the positioning of an analogue display indicator (needle) in relation to a scale (susceptible to parallax error and many misreading sources), data recording and transfer, its processing and storage.

Automatic readout based on computer vision systems is thus being worked out for analogue devices equipped with no digital interface. It involves advanced digital image processing to eliminate a human eye from this process and replace it with just a camera-software duet. In case of DUT (Device Under Test) fitted with a digital display, an OCR (Optical Character Recognition) algorithm is enough to flawlessly read out the meter indication, especially when combined with a neural network approach for automated learning [1] as well as statistical processing of raw OCR results, which may be easily implemented for instance in a graphical programming language like LabView [2]. However, in case of “truly” analogue meters fitted with an indicator gauge, the task is not so trivial as the image processing algorithms must deal with location of several sets of line sections and arcs with high level of details, which are difficult to be categorized.

Some solutions for performing automated computer-assisted readings of such analogue meters have been already proposed. Alegria and Serra presented a system performing readout of analogue meters realized by means of a video camera and a dedicated computer program. Frames taken by the camera were analyzed in software according to a general algorithm consisting of 2 main parts. Initially, the center of needle rotation, scale arc and scale limits were localized in order to move to the second part of the algorithm, which was responsible for the actual calibration i.e. location of the actual needle position and its indication. The proposed algorithm made the extensive use of background subtraction and Hough transform for localization of lines. The results presented in the cited paper were influenced with just 0.1% total reading error, however the depicted algorithm did not take into consideration the parallax effect and its influence on the measurement and its uncertainty. Moreover, as the described algorithm was heavily exploiting background subtraction, the correction of parallax effect could not have been performed because shadow or mirror reflection of the needle was completely discounted [3].

De Lima *et al.* presented a computer vision system which also utilized similar concepts. Localization of a needle was made by the edge detection and Hough transform. Values were read by comparing the angle of pointer deflection with the maximal deflection values. The results presented in the paper were said to be flawless and have 100% accuracy, which was itself strongly discussable. Moreover, the ROI used for localization of the needle did not encompass its shadow or mirror reflection therefore the parallax effect was disregarded [4].

The problem of the parallax error seems to be therefore a prime drawback of the scientific work performed so far in this field. An all-digital solution of this problem is thus addressed in the presented paper, based on the Hough transform used to extract lines from an image, additionally enhanced with an extensive statistical processing of its raw results based on the multiply histogram analysis. The algorithm was tailored for the readout of high-accuracy analogue meters with a needle indicator, which were commonly fitted with a mirror for a human user to correct for the parallax effect. An attempt to use the algorithm implementation for semi-automatic calibration of an analogue voltmeter is also presented.

2. Apparatus

A simple automated vision system, used in the experiments, is schematically shown in Figure 1.

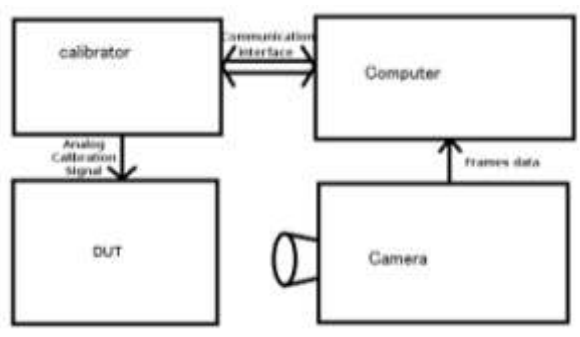

Fig. 1. Simplified diagram of the automated test set-up

It consisted of a digitally-controlled calibrator (Inmel 7000, Inmel), which was wirelessly interfaced via a Bluetooth-RS232 adapter to a personnel computer (PC). An analogue signal, generated by the calibrator according to the commands sent remotely by a PC, was routed to a DUT (analogue indicator meter). The calibrator was used to simulate the "measured" signal as accurately as it was feasible in order to disregard the test signal uncertainty or instability. A digital camera of a mobile phone (HTC Desire, HTC) was then used to dynamically acquire images of the DUTs scale at 30 f-p-s and 1280×720 resolution. The mobile phone was exercised in order to make the system mobile in the future. The frames acquired by the camera were then transferred to the PC using a Wi-Fi link and IP Webcam software [5] allowing to use the smartphone in the IP camera mode. A specialized software, run on the PC, was responsible for supervising all the hardware elements of the system as well as performing the digital image analysis, which was the main goal of the investigations explained in details later in the paper.

3. Algorithm development

The algorithm used for performing the analysis of the DUT scale images was developed under the following assumptions:

- DUT must have a linear scale.
- DUT must be equipped with a mirror for effective parallax effect correction.
- DUT scale surface must be located perpendicularly to the optical axis of the camera.
- DUT mirror is not seriously recessed in relation to the scale.

The developed algorithm consisted of 4 principal steps:

1. preparation procedure;
2. positioning and alignment procedure;
3. raw needle line reconstruction;
4. parallax correction.

The preparation procedure was to be completed by the human user. During this step the operator was responsible for setting up vital parameters for the readout process:

- kind of the test signal (voltage, current etc.),
- minimal and maximal test signal values (as OCR of scale depictions was not performed),
- ROI encompassing meter indicator, scale and the mirror.

When the preparation step was completed, the positioning and alignment procedure was initiated, which was the first part of the automatic image data handling. Initially, raw frames received from the camera were processed using the canny edge detection algorithm. Then, the Hough transform was used to search selected ROI for 2 longest parallel lines. The mean line, calculated from those two lines, indicated the needle position. Such a process was repeated 3 times at the minimal, medium and maximal test signal magnitude (as illustrated in Figure 2), producing a set of 3 lines. Their intersection was treated as the center of needle rotation. Although in theory 2 lines would be enough for this purpose, the 3rd line was introduced to correct for eventual mistakes in localization of the center (related for instance to non-uniformity of the DUT scale or slight bending of the needle). The actual position of the rotation center was calculated as the mean value of 3 intersection points formed by 3 lines. As soon as the center of the needle rotation was automatically computed, the user was requested to indicate a proper radius of the circle (settled in the calculated center of rotation), which spanned over the meter mirror.

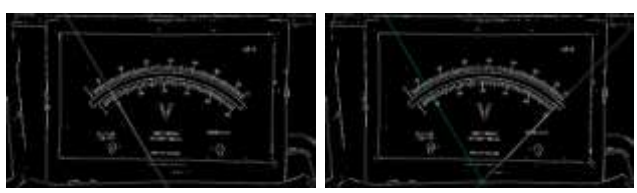

Fig. 2. Finding the needle position at: a) starting, b) maximal signal magnitude

When the position of the mirror was acquired, the start and end points of the scale were searched for, however this time correction of the parallax effect was introduced. Figure 3 illustrates a simple geometrical model used to calculate the exact position of the needle when its mirror reflection location was known.

The following symbols were introduced: P and P' – points of view (i.e. positions of the camera), O and O' – the needle and its reflection, H – distance between the camera and the scale (and the mirror), a – distance between the camera and the position directly above the needle, d_1 – distance of the needle from the point which camera see from position P' (not directly above the needle, where the parallax is present), d_2 – distance of the reflection from the mirror seen from the camera in position P' (not directly above the needle, where the parallax is present), h_1, h_2 – distance between the needle and its reflection in the mirror (we assume that $h_1 = h_2 = h$).

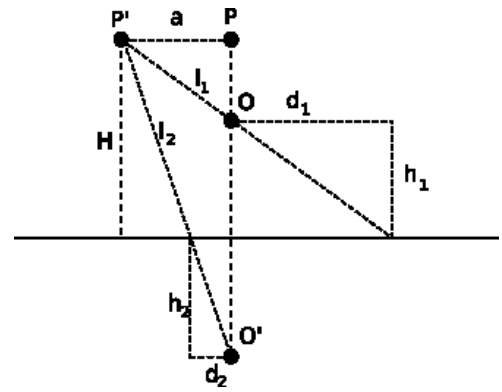

Fig. 3. Geometrical illustration of the parallax effect correction

Separations d_1 and d_2 (as it is shown in Figure 3) are related to each other according to the following formula:

$$\frac{d_1}{d_2} = \frac{H+h}{H-h} \tag{1}$$

In practice, the distance of the camera from the scale is much greater than the distance of the needle from the scale ($H>>h$), hence (1) may be simplified as:

$$\frac{d_1}{d_2} = \frac{H}{H} \tag{2}$$

which denotes that $d_1/d_2 = 1$ and therefore the correct position of the needle can be straightforwardly determined in the middle between the needle and its mirror reflection.

As soon as the accurate parallax-corrected extremal locations of the scale have finally been located, the main readout stage may be start off. In the test system, it involved setting a reference value, which was transmitted to the calibrator and then (after a specified delay, necessary to account for the calibrator latency and the needle inertia) a number of consecutive frames was analyzed in order to calculate the reconstructed meter readout.

As it was stated above, acquisition of a single readout of the meter needle position was performed using the two-step image analysis, consisting of:

1. finding a raw needle position,
2. finding its correct (parallax-adjusted) position.

In the first step, a single frame was considered. It was initially subjected to the cunny edge detection algorithm and then the Hough transform was applied in order to find all lines existing in the image (the threshold for line length determination was adapted automatically in this process). Then, only lines long enough to physically go through the direct neighborhood of the needle center of rotation were selected for further processing. The neighborhood was defined by a circumscribed circle of the triangle defined by trisection of lines used to localize the center of needle rotation.

The lines selected in this way were then combined into a single "mean" line located in the middle between them, which finally represented the raw needle position.

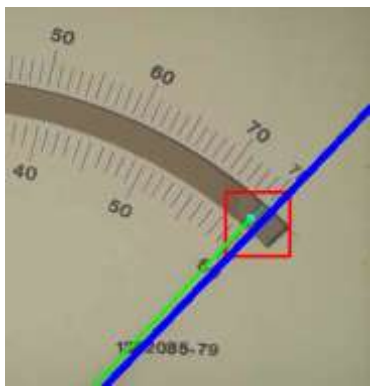

Fig. 5. Section of a frame used for parallax-correction analysis: red square indicates ROI in which the raw position of the needle (blue line) and its parallax-corrected location (green line) are searched

The second step of the reconstruction involved a parallax correction. A small square ROI, centered at the needle-mirror line crossing point, encompassing the needle reflection was cut out from the frame (Figure 5) and an image manipulation was performed in order to obtain its binary representation. Such an operation was repeated and 10 binary images were accumulated together to form a "mean" binary image in order to eliminate various instabilities (e.g. resulting from the pixel noise, minute lighting variations and the camera performance). The averaging depth of 10 frames was chosen through trial and error as the smallest one producing satisfactory results. The resulting time- and spatially-averaged binary image was then searched for the needle and its mirror reflection to calculate the parallax-corrected position of the needle, according to (2).

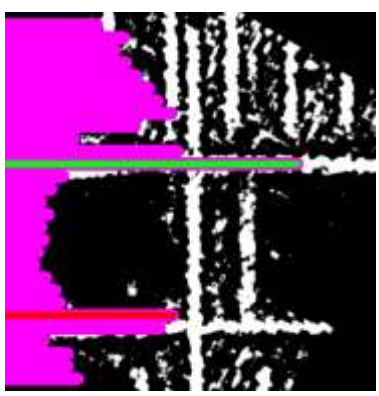

Fig. 6. Parallax correction: a rotated "mean" binary frame combined with its perpendicular histogram, indicating position of the mirror edges (marked by green and red lines)

However, because the size of the zoomed part of the image encompassing the needle and its reflection was very limited, well known edge detection algorithms were not applicable, as they yielded incorrect results. An innovative, purpose-tailored edge searching algorithm to locate the needle and its reflection was thus worked out. It was based on the double histogram analysis method (reducing the 2D image analysis into 1D problem) and made use of the observation, that the needle and its reflection both possessed a certain width and thus consisted of 2 parallel edges, which dominated the histogram, when it was built along the direction of the needle line. Though, the "mean" binary image also contained edges of the mirror, which had to be cleared before searching for the needle and its reflection. The "mean" binary image was thus first rotated in order to orient the "raw" needle trace vertically and the first histogram was computed along the direction perpendicular to the needle line (Figure 6 illustrates a rotated "mean" binary image with its "perpendicular" histogram superimposed and marked in pink). As the mirror area was significantly brighter than its edges, the first histogram was composed of two strong maxima (corresponding to the edges of the mirror, marked in Figure 6 as red and green lines) separated by a characteristic caldera-like valley (corresponding to the mirror area).

A segment of the "mean" binary image between the horizontal histogram extrema was then extracted and the second histogram was calculated for this truncated image along the direction parallel to the needle line (Figure 7 shows the "mean" binary image cleared from the mirror edges with a superimposed "parallel" histogram marked in blue). The second histogram contained only two strong maxima representing the needle and its reflection, thus the parallax-corrected position of the needle was easy to find according to (2), which is illustrated in Figure 7 by a purple line.

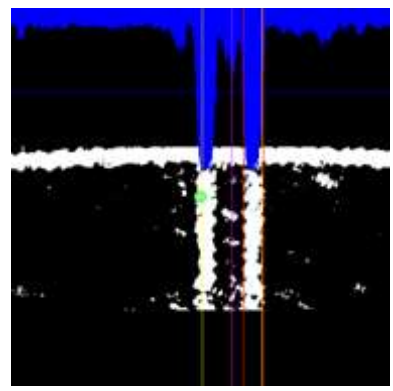

Fig. 7. Parallax correction: a rotated "mean" binary frame cleared from mirror edges with "parallel" histogram superimposed. Purple line indicates a corrected position of the needle

Having found the parallax-corrected needle line position, the final step was to recalculate it into the exact gauge indication, assuming that all lines (corresponding to the needle and the beginning and end of the scale) intersected at the center of the needle rotation and that the gauge scale was angularly linear.

4. Implementation-related problems

The above algorithm was implemented using C++ language (Microsoft Visual Studio C++ 12.0) and open source OpenCV computer vision library ver. 2.49 [6]. Although the presented image analysis process was simple in its idea, certain problems were encountered during its preliminary laboratory tests.

As it turned out from the experiments, a noteworthy problem was related to a requirement for capturing frames with equivalent exposition parameters. It required constant, uniform and shadow- as well as reflection-free lighting of the scene, uninfluenced by peripheral light sources and shadows. As it turned out, a combination of 2 pieces of white 3 W stabilized LED lamps and a light tent was not enough to completely eliminate the problem of uneven brightness and contrast in the long frame streams (although the light tent successfully eliminated light source reflections in the scale glass and the mirror). The influence of uneven hardware lightning conditions was finally minimized using the adaptive method for image binarization implemented in OpenCV Library as the *dst*() function, which transformed a grayscale image to its binary (two-color) representation according to the following formulae [7]:

$$dst(x,y) = \begin{cases} maxValue & if\ src(x,y) > T(x,y) \\ 0 & otherwise \end{cases} \quad (3)$$

A specific mechanical construction of the tested analogue meters was also a drawback. The reflection of the mirror boundary observed near the extreme ends of the scale significantly influenced the localization of a correct position of the needle, when it was located near the extreme terminations of the scale. For instance, ROI shown in Figure 5 actually contained 3 lines: the needle (marked with a blue line), its mirror reflection (located on its left hand side) as well as unwanted reflection of the scale end edge. This third "extra" line had to be removed before searching for the needle and its reflection line representation as it was significantly affecting the obtained reconstruction results. The problem was successfully solved by automatically extending ROI selected by the user during the preparation step. The extension was only applied when the raw needle position was within 5% of the scale extrema. An exemplary frame obtained using such processing is presented in Figure 8 together with its histogram.

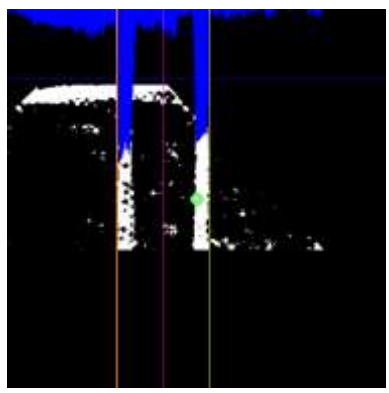

Fig. 8. Exemplary frame showing parallax-corrected needle localization near the end of the scale with extended ROI

Another problem was related to correct localization of edges. The solution which was effectively applied was based on searching for the greatest differences ("steps") in the image histogram and thus localization of pairs of the so-called rising (where the difference was maximal and positive) and falling line edges (located at most negative differences). However, even such an approach to distinguish the position of the needle and its reflection was not 100% effective when the objects to be discriminated were located very close to each other i.e. when the needle was located in the middle region of the scale. In such a case, it was feasible to locate a pair of the most distant edges (one rising and one falling) and reconstruct the line location in the middle between them.

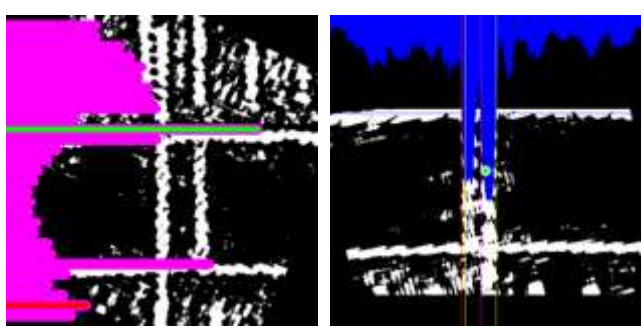

Fig. 9. Searching for the needle and its reflection lines on a misinterpreted image: a) misinterpreted falling edge used to trim the image, b) incorrectly trimmed and binarization-distorted image used for parallax-correction

Despite all the applied correction techniques, there still appeared some misprocessed frames (an exemplary frame pair is shown in Figure 9), which however resulted only in ineffective (in most cases negatively biased) correction of the parallax. It seemed that the main source of such problematic images was related to the image binarization step, which produced the distorted line-representing regions (blurred or eroded). Such errors were encountered infrequently (approximately in 0,2-0,4% frames) however they might be responsible for the increase in the total red-out error observed when the needle was located near the middle of the scale (where paradoxically the parallax was the least influencing factor).

5. Exemplary application

As an illustration of the performance of the developed laboratory set-up and the algorithm, their application to an automated analogue voltmeter (type Mera LE-3, serial number: 1302085.79, class 1, range 0-60 V DC), for which an official calibration certificate was issued (by Główny Urząd Miar in Wroclaw) is presented. A reference voltage was generated by the calibrator. A digital value, calculated using the developed image analysis algorithm and corresponding to the analog meter indication was obtained and such an operation was reiterated to cover all the specified calibration points for a specified number of repetitions. A set of digital values was then further statistically processed to calculate the calibration parameters (error, uncertainty) according to the common procedure [8, 9] and finally a calibration report was automatically generated. The results of the calibration performed using the digital image processing are presented in Table 1.

Tab. 1. Results of digital image processing calibration

Reference value, V	Read value, V	Uncertainty, mV	Error, V
13.0000	12.9174	111.5280	0.0826
26.3333	27.0310	31.7502	0.6977
39.6667	40.1192	102.1100	0.4525
54.0000	53.9271	88.5941	0.0729

The results given in Table 1 implied that the tested voltmeter was characterized by errors which were the highest near the middle of the scale. This observation differs from the commonly expected feature of meters fitted with an analogue gauge, in which the reading error is reduced towards the upper end of the scale. The reason for such a result cannot be explicitly identified, it may be however related to the hardware of the tested meter (e.g. a local non-linearity of the scale and the gauge mechanism). The uncertainty of the single reference value readout was reasonably small (<0,1% i.e. well beyond the tested meter class), which indicated that the applied image analysis algorithm yielded steady and trustworthy readout values. The values delivered by the image processing algorithm were also almost an order of magnitude better than the conventional human worker error (the uncertainty of readings performed visually by a usual human worker in the case of analogue meters can only be limited to a half of the scale segment, which in the case of the tested certified meter was 0,5 V). Therefore, the proposed method was effectively more than equivalent to human reading of a scale.

Tab. 2. Certified results of calibration

Reference value, V	Read value, V	Uncertainty, V	Error, V
10.00	9.96	0.02	0.04
20.00	19.98	0.02	0.02
30.00	29.86	0.03	0.14
40.00	39.89	0.03	0.11
50.00	49.85	0.03	0.15
60.00	59.83	0.04	0.17

Table 2 presents the results of the official calibration as contained in the meter certificate. The certified results of the calibration are almost an order of magnitude more "optimistic"

than those obtained using the presented image processing method. Unfortunately, the data presented in Table 1 and 2 cannot be explicitly compared because the methodology and the equipment applied by the certification authority were not known.

6. Conclusions

The proposed image processing algorithm was applicable in automatic location of the needle and readout of its position in the analogue measuring equipment fitted with an indicator gauge. Its computer implementation produced the results which were almost an order of magnitude better than the results obtained by an average person reading a scale visually. The presented approach may be thus applicable in automation of measuring processes, where the constant monitoring of analogue gauges is required and their replacement by truly-digital ones is not judged technically or economically.

Practical implementation of the presented algorithm, heavily-based on open source computer vision library (OpenCV) currently available for Android OS and application of a mobile phone as a camera, makes it possible to easily transform the presented solution into a totally mobile application e.g. by porting the algorithm to Java and using just a smartphone (or a tablet) as the combined image capturing and processing center. Together with wireless BlueTooth or Near Filed Communication functionality built into modern mobile gadgets, taking analogue measurements and calibration would be possible using an autonomous, portable and popular device.

7. References

[1] Andria G., Cavone G., Fabbiano L., Giaquinto N., and M. Savin: Automatic Calibration System for Digital Instruments without built-in Communication Interface. XIX IMEKO World Congress Fundamental and Applied Metrology, September 6−11, 2009, Lisbon, Portugal.
[2] Pociecha D. M.: Development of the automatic stand for the measurement devices calibration using advanced image processing, MSc dissertation, Wrocław University of Technology, 2014.
[3] Alegria F. C., and Serra A. C.: Automatic Calibration of Analog and Digital Measuring Instruments Using Computer Vision, IEEE Trans. on Instrumentation and Measurements, vol. 49, no. 1, 2000.
[4] de Lima D. L., Pereira G. A. S., de Vasconcelos F. H.: A Computer Vision System to Read Meter Displays. 16th IMEKO TC4 Symposium Exploring New Frontiers of Instrumentation and Methods for Electrical and Electronic Measurements, Sept. 22-24, 2008, Florence, Italy.
[5] https://play.google.com/store/apps/details?id=com.pas.webcam, hyperlink valid on 12.10.2015.
[6] http://opencv.org/, hyperlink valid on 12.10.2015.
[7] http://docs.opencv.org/modules/imgproc/doc/miscellaneous_transformations.html?highlight=adaptivethreshold, hyperlink valid on 12.10.2015.
[8] Lisowski M.: Podstawy metrologii. Oficyna Wydawnicza Politechniki Wrocławskiej, 2011.
[9] Taylor B. N., Kuyatt Ch. E.: Guidelines for Evaluating and Expressing the Uncertainty of NIST Measurement Results. NIST Technical Note 1297, United States Department of Commerce Technology Administration, National Institute of Standards and Technology, 1994.

Received: 09.08.2015 Paper reviewed Accepted: 02.10.2015

Dominik POCIECHA MSc, eng.

He obtained the BSc eng. degree in Automatic Control from Silesian University of Technology (2011) and the MSc degree in Electrical Engineering from Wroclaw University of Technology (2014). He is currently pursuing his PhD degree in electrical engineering at Wroclaw University of Technology. His scientific interest is related to electrostatic phenomena, instrumentation and computer control.

e-mail: dominik.pociecha@pwr.edu.pl

Paweł Żyłka PhD, eng.

He obtained the MSc degree in instrumental analytical chemistry from Glasgow Caledonian University (1995) and the MSc degree in materials science as well as the PhD degree in electrical engineering from Wroclaw University of Technology (WUT, 1996 and 2002, respectively). Since 1996, he has been employed at the Department of Electrical Engineering Fundamentals at WUT. His scientific interest is currently focused on bioinspired high voltage engineering, electroactive polymers and instrumentation.

e-mail: pawel.zylka@pwr.edu.pl